Splay fault branching from the Hikurangi subduction shear zone: Implications for slow slip and fluid flow

A. Plaza-Faverola[1,2], S. Henrys[1], I. Pecher[1,3], L. Wallace[1,4], and D. Klaeschen[5]

[1]GNS Science, Lower Hutt, New Zealand, [2]Now at CAGE—Centre for Arctic Gas Hydrate, Environment and Climate, Department of Geology, UiT—The Arctic University of Norway, Tromsø, Norway, [3]School of Environment, University of Auckland, Auckland, New Zealand, [4]University of Texas Institute for Geophysics, Austin, Texas, USA, [5]GEOMAR, Helmholtz Centre for Ocean Research, Kiel, Germany

Abstract Prestack depth migration data across the Hikurangi margin, East Coast of the North Island, New Zealand, are used to derive subducting slab geometry, upper crustal structure, and seismic velocities resolved to ~14 km depth. We investigate the potential relationship between the crustal architecture, fluid migration, and short-term geodetically determined slow slip events. The subduction interface is a shallow dipping thrust at <7 km depth near the trench and steps down to 14 km depth along an ~18 km long ramp, beneath Porangahau Ridge. This apparent step in the décollement is associated with splay fault branching and coincides with a zone of maximum slip (90 mm) inferred on the subduction interface during slow slip events in June and July 2011. A low-velocity zone beneath the plate interface, updip of the plate interface ramp, is interpreted as fluid-rich overpressured sediments capped with a low permeability condensed layer of chalk and interbedded mudstones. Fluid-rich sediments have been imbricated by splay faults in a region that coincides with the step down in the décollement from the top of subducting sediments to the oceanic crust and contribute to spatial variation in frictional properties of the plate interface that may promote slow slip behavior in the region. Further, transient fluid migration along splay faults at Porangahau Ridge may signify stress changes during slow slip.

1. Introduction

Fluid flow and seafloor seepage in continental margins have well established implications for the Earth's global climate [e.g., *Etiope*, 2009; *MacDonald et al.*, 2002; *Svensen et al.*, 2004], for prediction of hydrocarbon accumulations [*Gay et al.*, 2003; *Hovland et al.*, 2010], and for marine hazard assessment [*Bugge et al.*, 1987; *Judd and Hovland*, 2007]. Although fluid expulsion from marine sediments to the seafloor is frequently manifested as pockmarks, mounds, mud volcanoes, or as direct seepage along faults [*Barnes et al.*, 2010; *Berndt*, 2005; *Judd and Hovland*, 2007; *Plaza-Faverola et al.*, 2014; *Saffer and Bekins*, 1999; *Westbrook*, 1991], tracking the origin of these fluids remains challenging but necessary for a full account of the fluid budget in continental margins.

In accretionary prisms, structural deformation and fluid migration as a consequence of burial and compaction have a complex history of interactions [e.g., *Moore et al.*, 2011; *Moore and Vrolijk*, 1992; *Westbrook*, 1991]. Loading, heating, and deformation in active tectonic regimes drive high fluid pressures and fluid flow [*Moore et al.*, 2011]. Pore fluid pressure buildup associated with fluid accumulation and migration can influence the style of deformation and faulting [*Bolton and Maltman*, 1998; *Moore et al.*, 2011]. Maintaining a critical taper during lateral growth of an accretionary wedge may result in fluid-rich sediment underplating, facilitating splay fault evolution [*Audet*, 2010]. If the interplay between splay and megathrust fault rupture, underplating, and fluid pressure does contribute to the diversity of fault slip behavior at subduction zones, then determining the geometry of the plate interface and overlying crust is critical to understanding how plate boundary displacements are accommodated.

Along the Hikurangi subduction margin of New Zealand (Figure 1), slow slip events (SSEs) are identified from continuous GPS observations [*Wallace and Beavan*, 2010]. SSEs are episodic creep events on the subduction interface and are inferred to be associated with large amounts of slip (a few to tens of cm) lasting days to years. Hikurangi SSEs often have comparatively large amounts of slip (typically 10–30 cm) with a
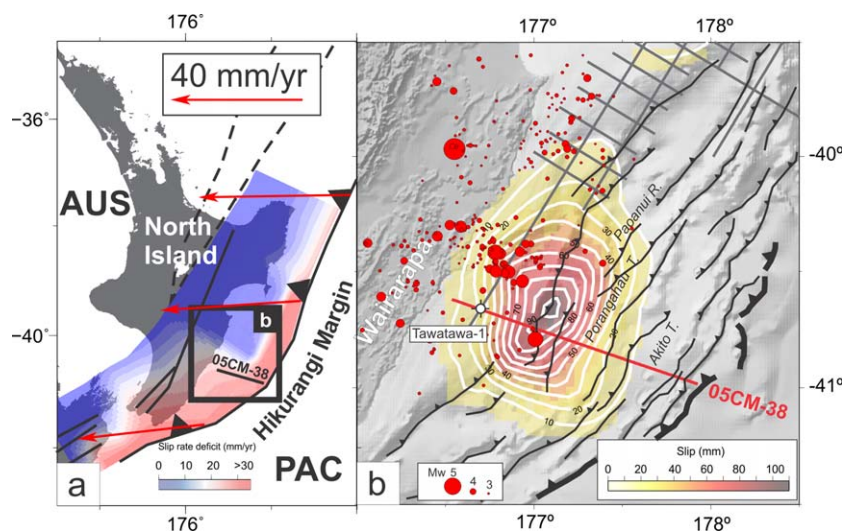
Figure 1. Regional tectonic setting of the East Coast of the North Island of New Zealand. (a) Slip rate deficit distribution at the plate interface [*Wallace and Beavan*, 2010]. Red regions are where the plate interface is interseismically locked. Red arrows show the relative convergence vector between the Pacific and Australian Plates. PAC, Pacific Plate and AUS, Australian Plate. (b) Location of the investigated seismic reflection line 05CM-38 (red line). Other seismic reflection data coverage of the 05CM survey are shown in grey lines. Cumulative slip on the interface in the 2011 East Coast slow slip event (SSE) sequence from *Wallace et al.* [2012] is represented in yellow to brown colors (white contours labeled in millimeters). Red filled circles are earthquake epicenters in the depth range 3–20 km and magnitude greater than 3, from January 2000 to January 2016 (GeoNet catalog: http://quakesearch.geonet.org.nz/).

Mw equivalent to 6.0–7.0 and durations varying from weeks to a year [*Bartlow et al.*, 2014; *Wallace and Beavan*, 2010]. At southern Hikurangi, most of these SSEs occur at the downdip transition (>30 km depth) from interseismic locking to steady aseismic creep [*Wallace and Beavan*, 2010, Figure 1]. In contrast, shallow SSEs (<5–15 km) are observed at the central and northern Hikurangi margin, in a region where most of the shallow subduction interface is dominated by aseismic creep but may host patches that are interseismically locked [*Wallace et al.*, 2016]. In 2011, a short-term SSE sequence occurred, offshore Wairarapa, surprisingly within the previously interseismically locked portion of the plate interface but in a region that is considered partially coupled and within the along strike-transition from deep to shallow coupling [*Wallace et al.*, 2012]. The 2011 sequence is also near a zone of heat flow anomalies inferred from pronounced upwarping of BSRs [*Pecher et al.*, 2010; *Crutchley et al.*, 2011] and active seafloor venting [*Bialas*, 2011]. Many studies suggest that elevated fluid pressures (i.e., near lithostatic) promote SSEs by reducing effective stresses along fault planes [e.g., *Audet*, 2010; *Ito et al.*, 2005; *Liu and Rice*, 2005; *Song et al.*, 2009]. *Saffer and Wallace* [2015] show that many regions of shallow slow slip events (e.g., <15 km deep) are closely associated with expected high fluid pressures from compaction and dewatering of subducted sediments. It is also possible that strain due to SSEs can drive fluid flow through overlying sediments, both by diffusion or through fractures/faults [*Brown et al.*, 2005; *Davis et al.*, 2011].

Analysis of seismic P wave velocities as indicators of anomalous pore-fluid pressures can contribute to understanding the role of fluid distribution in controlling styles of fault slip [e.g., *Ito et al.*, 2005; *Peng and Gomberg*, 2010; *Song et al.*, 2009]. Geochemical, geological, and geophysical studies from many subduction margins suggest that significant amounts of fluids involved in subduction processes are concentrated in sedimentary layers underlying the décollement, leading to zones of excess pore-fluid pressures [e.g., *Ellis et al.*, 2015; *Moore et al.*, 2011; *Saffer*, 2003]. At the northern Hikurangi margin, seismic reflection data reveal diverse plate interface properties, including zones of high-amplitude reflectivity coinciding with the source area of some SSEs [*Bell et al.*, 2010]. The high-amplitude zones are interpreted as fluid-rich underplated sediments, while intervening lower amplitude zones, and nonreflective areas interpreted as subducting seamounts.

In this study, we explore the relationship between slow slip, fluid flow, and geometry of the subduction zone in the region of the short term (∼2–3 weeks duration) 2011 slow slip events at the Hikurangi margin. Specifically we integrate P wave velocity and waveform modeling with complimentary structural analysis

[*Ghisetti et al.*, 2016] derived from high quality prestack depth-migrated multichannel seismic reflection data that crossed close to the maximum slip for the 2011 SSE sequence (Figure 1). We suggest a conceptual model to provide an explanation to the observed correlation between splay fault branching within the subduction shear zone, overpressured fluid-rich sediments, and slow slip occurrence.

2. Prestack Depth Migration Data

We conducted prestack depth migration (PSDM) along seismic profile 05CM-38, part of a 2D survey lead by the New Zealand Ministry of Business, Innovation and Employment (formerly MED, Ministry of Economic Development) along the East Coast of New Zealand North Island. Time migrated versions of this seismic profile have been the subject of detailed studies of shallow structures related to fluid flow and hydrates in the Porangahau Ridge region [*Crutchley et al.*, 2011], as well as studies of the subduction interface [*Barker et al.*, 2009]. Data consist of 960 channels with a maximum offset of 12 km. The source was a 4140 m^3 airgun array. Shot interval was 37.5 m and sampling rate 2 ms.

We reprocessed the seismic profile focusing on multiple removal and depth migration in order to image deeper structures linking deep sourced fluids with the gas hydrate stability zone (GHSZ). Premigration processing (supporting information Table S1) included bandpass filtering, seafloor reflection-based multiple elimination (SRME), Tau-P deconvolution, radon multiple removal, and CDP binning at 12.5 m. The PSDM approach implemented is that described by *Plaza-Faverola et al.* [2012] and similar to the approach by *Hoffmann and Reston* [1992] and *Kopf* [1999]. The PSDM is performed iteratively, using updated *P* wave velocity models (V_p) to improve subsequent migrated images. Depth conversion, energy depth focusing analysis, velocity model smoothing, and ray tracing are main routines in the flow, performed iteratively until the preferred image of the structures is obtained. Progressive minimization of the normalized errors (α) and focusing of the reflection energy around $\alpha = 1$ (supporting information Figures S1.1 and S1.2) determines the choice of the resulting image. We performed nine iterations for line 05CM-38. However, after iteration 5 the resulting image appeared already robustly constrained and only small refinements were observed (Figure 2 and supporting information Figure S1.3).

3. Interpretation

The convergent margin offshore northern Wairarapa lies at the southern end of the Tonga-Kermadec-Hikurangi subduction zone, where thick 120 Ma oceanic crust of the Hikurangi Plateau (Pacific Plate) is being subducted westward beneath the Australian Plate. Here the Pacific Plate motion of ∼42 mm/yr is partitioned between margin-normal slip on the subduction thrust, accounting for 80% of the convergence in the last 5 My [*Nicol and Beavan*, 2003], margin-normal shortening, strike-slip faulting, and vertical-axis fault-block rotations. Margin-normal shortening in the overriding plate accounts for 6–19% of convergence [*Nicol and Beavan*, 2003]. Shortening is mainly accommodated by folding and thrust faulting offshore [*Barker et al.*, 2009; *Barnes et al.*, 2010; *Barnes and Mercier de Lepinay*, 1997; *Davey et al.*, 1986; *Lewis and Pettinga*, 1993]; imaged on line 05CM-38 as a 150 km wide deformed prism. The accretionary wedge along this part of the Hikurangi margin includes an inner wedge of deforming Late Cretaceous and Paleogene rocks, greater than 10 km thick, and an outer wedge of late Cenozoic accreted trench-fill turbidites [*Barnes et al.*, 2010]. The outer wedge is primarily composed of a deforming cover sequence of Miocene to Recent shelf and slope basin sediments up to 6 km thick and is characterized by low taper (∼3°) with average surface slope of about 1°. Deformation in the outer wedge, offshore Wairarapa, is accommodated principally by imbricate thrusts that young eastward toward the toe and sole into a reflection horizon that defines a décollement, separating the deforming accretionary sediments above from undeformed sedimentary reflectors on the downgoing plate beneath [*Barker et al.*, 2009; *Ghisetti et al.*, 2016].

Our interpretation of the seismic stratigraphy of 05CM-38 (Figure 2) is based on previous descriptions by *Barnes and Mercier de Lepinay* [1997], *Barnes et al.* [2010], *Plaza-Faverola et al.* [2012] and extended to our study from *Ghisetti et al.* [2016]. Main structural features imaged in the ∼120 km long prestack depth-migrated section include the plate interface with associated subducted sedimentary zone, a step-down in
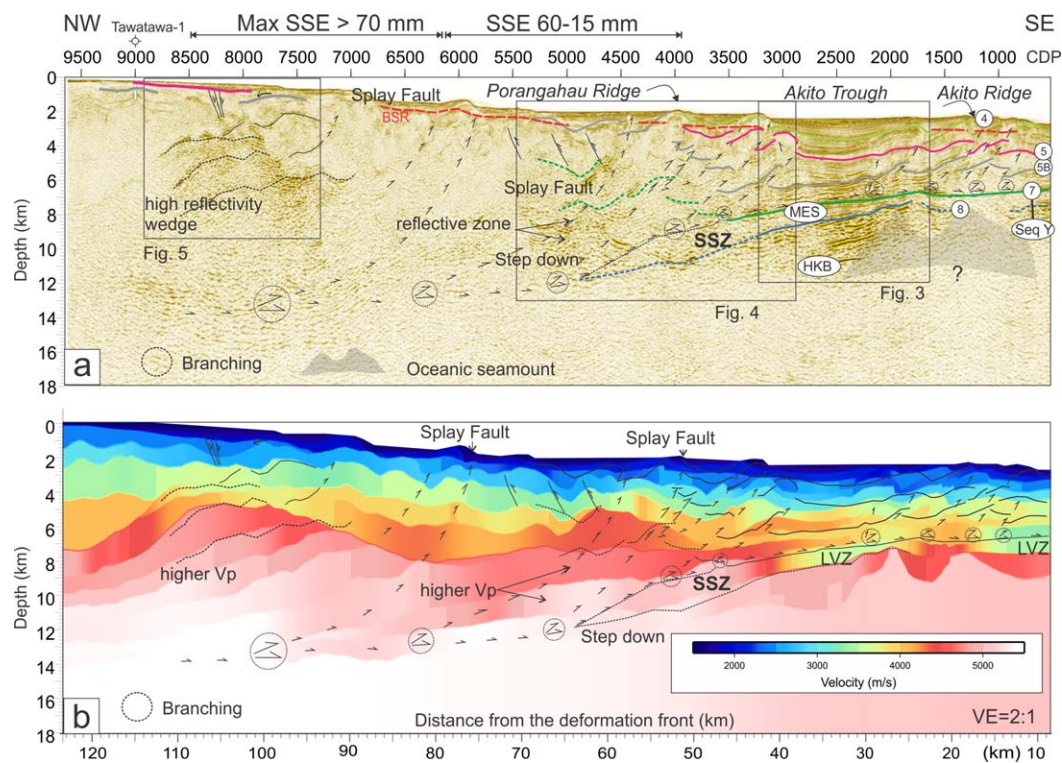
Figure 2. (a) Prestack depth-migrated seismic transect along profile 05CM-38 resolving the depth of the subduction interface from ∼7 to 14 km. The interpreted seismic reflections are identified from *Barnes and Mercier de Lepinay* [1997], *Barnes et al.* [2010], *Plaza-Faverola et al.* [2012], and adapted from *Ghisetti et al.* [2016]. HKB, the top of the Hikurangi margin basement; MES, Mesozoic sediments; Sequence Y (Seq. Y) is a condensed section coinciding with the décollement. Faults and splay fault branching are shown in black arrows. The extent of slow slip events (SSEs) from 2011 (in millimeters) is projected; SSZ, subducted sediment zone; BSR, bottom simulating reflector. Vertical exaggeration 2:1. (b) *P* wave velocity model used for prestack depth migration. The "*X*" axis denotes distance from the deformation front. In general, velocities have a picked semblance-associated error <5%. Details of the processing sequence are given in supporting information.

the décollement possibly accommodating sediment underplating, and splay fault branching at the décollement.

3.1. Seismic Character of the Subducted Sediment Zone

The décollement across the Hikurangi margin is well resolved in the outer accretionary wedge, east of Porangahau Ridge and beneath the Akito trough at 7 km depth (Figures 2 and 3). The décollement is coincident with, or lies above, Reflector 7 which has been inferred as the boundary between the Miocene sediments and the underlying reflective condensed Late Cretaceous-Early Oligocene (70–32 Ma) sediments (sequence Y of *Davy et al*. [2008]). The latter are underlain by a weakly reflective unit that is inferred to comprise Cretaceous sedimentary rocks (MES of *Davy et al*. [2008], 100–70 Ma in age). The décollement exhibits a step down near CDP 4200 (50 km from the deformation front) forming a ∼8 km long ramp, dipping on average ∼20°, which soles to a nearly horizontal décollement at 13–14 km depth (Figure 2 and supporting information Figure S1.3). This part of the décollement appears to coincide approximately with the landward projection of Reflector 8, the top of the Early Cretaceous Hikurangi Plateau oceanic volcanic sequence (HKB of *Davy et al*. [2008]). We refer to the subducting Pacific Plate sedimentary sequence (between Reflectors 7 and 8) as the subducted sediment zone (SSZ).

The SSZ experiences a thickness increase westward below Porangahau Ridge (i.e., downdip) with an average thickness of 2 km (Figures 2 and 3), and is well imaged beneath the Akito Trough and ridge (Figure 3). The upper boundary of the SSZ (coinciding with Reflector 7), toward the deformation front, is highly reflective and dips westward ∼3.5°. It shows reverse polarity at discrete locations where the zero phase wavelet has been preserved and can be compared with the seafloor reflection wavelet (Figures 3d and 3e). We interpret that the décollement coincides with Reflector 7 to the east of Porangahau Ridge and that extends to the deformation front beyond the eastern end of line 05CM-38 [*Ghisetti et al.*, 2016].
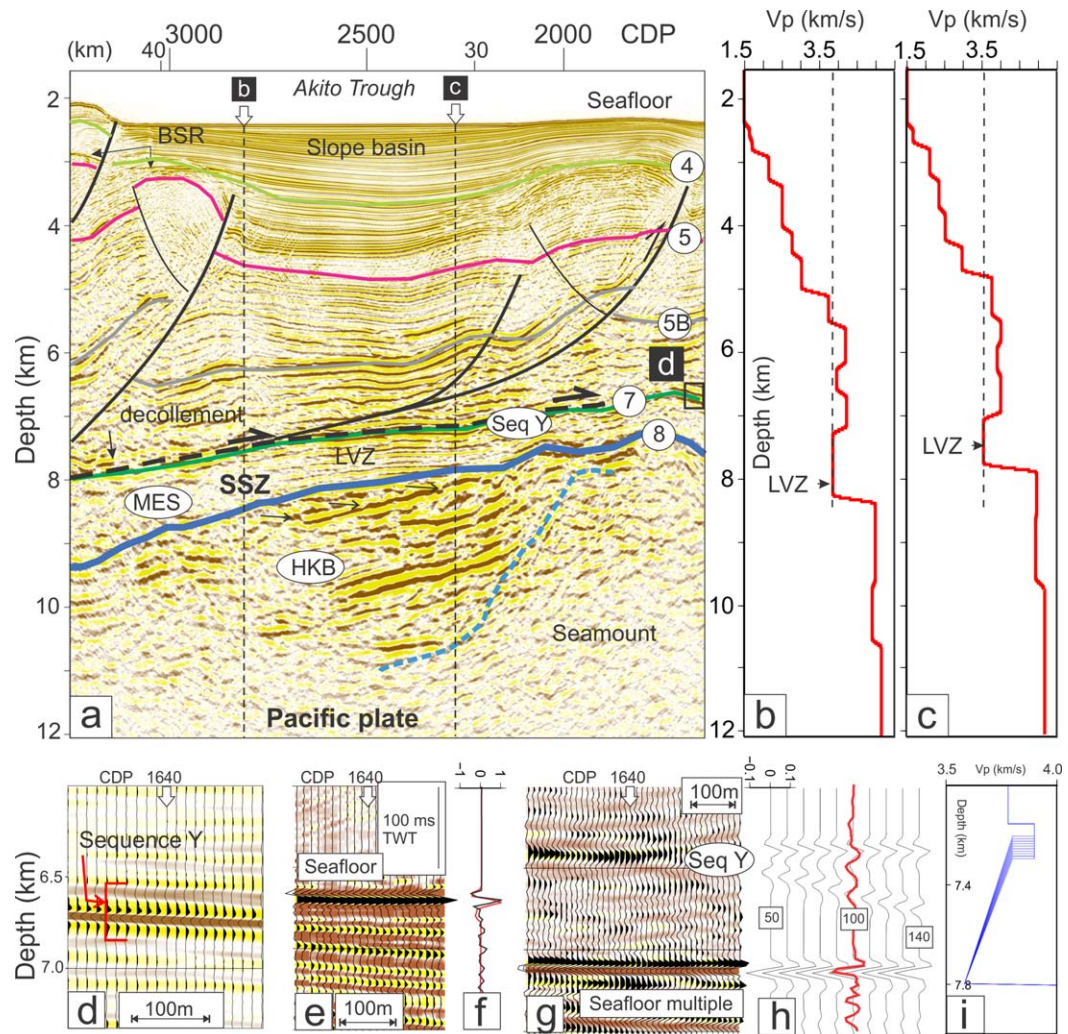
Figure 3. (a) Enlarged seismic image between CDP 1600 and 3260 (km 24–42). Interpreted faults and seismic reflections are from Figure 2. Distinctive bright reflections are identified within the subducted sediment zone (SSZ) where a low-velocity zone (LVZ) is well resolved by the semblance focusing velocity analysis. Reflector 7 is interpreted as the top of sequence Y [*Davy et al.*, 2008; *Wood and Davy*, 1994]. Plots (b) and (c) show the magnitude of the *P* wave velocity (V_p) inversion within the LVZ. Plot (d) shows polarity of the reflection at the top of the SSZ in comparison to the seafloor polarity. The brightest pick (yellow) in Figure 3d is inferred to be top of sequence Y, a potential seal for fluid from underthrusting sediments [*Plaza-Faverola et al.*, 2012]. Plot (e) is the time migrated near zero-offset traces enlarged around the seafloor (vertical axis is two-way travel time (TWT)). (f) Red single trace at CDP640 and matching synthetic seismogram of seafloor reflection (black). (g) Time migrated near zero-offset traces in a 300 ms window encompassing sequence Y, 120 ms above the seafloor multiple. (h) Red single trace at CDP640 and matching synthetic seismograms of V_p 3.9 km/s single layer that thickens from 50 to 140 m left to right (black). (i) Velocity models used in calculations of synthetic seismograms; constant density of 1.1 Mg/m^3 and $Qp = 200$. The best match of synthetic to observed data is for sequence Y to be 100 m thick.

3.1.1. Waveform Characteristics of Reflector 7

We investigate the waveform characteristics of Reflector 7 and the condensed Late Cretaceous-Early Oligocene reflection interval (sequence Y) to determine its thickness and the reflection coefficients across the plate interface. We carry out one-dimensional forward synthetic modeling [*Mallick and Frazer*, 1987] of simplified models of sequence Y and compare these to time migrated near zero-offset trace coda from raw 05CM-38 CDP sorted data.

Only limited portions of 05CM-38 show Reflector 7 above the seafloor multiple. We did the waveform analysis between CDPs 1600 and 1700 where we are confident that the wavelet amplitudes of sequence Y are not masked by multiple energy (Figure 3g). The wavelet amplitudes for Reflector 7 vary laterally on zero-offset traces and are highest near the eastern end of 05CM-38, but consistently show a "double peak" comprising a positive peak, the same polarity as the seafloor, followed by a negative peak in depth-migrated

images and near-trace raw data (Figures 3d and 3h). This signature is consistent with a thin high-velocity layer (3.9 km/s) of positive-polarity reflection coefficient top (0.017) and negative-polarity base (−0.013) overlying a low velocity layer (LVL) with velocity gradient of 3.8 km/s at the top and ∼3.5 km/s at the base. The base of the LVL lies below the seafloor multiple but, constrained by our PSDM to about 0.5 km thick. We varied the thickness of the high-velocity layer between 50 and 140 m with the best match between synthetic and observed data being 100 m thick (Figures 3h and 3i). In our synthetic modeling, we kept density constant (1.1 Mg/m^3) and used quality factor (Qp), of 200 for sedimentary layers. Sequence Y is widely recognized [*Barnes et al.*, 2010; *Bland et al.*, 2015; *Davy et al.*, 2008; *Ghisetti et al.*, 2016; *Plaza-Faverola et al.*, 2012] and tied to borehole data from the eastern edge of the Hikurangi Plateau at ODP site 1124, where it comprises Late Cretaceous-Early Oligocene nannofossil chalks and alternating mudstones [*Davy et al.*, 2008]. The resolution of 05CM-38 data is not sufficient to determine if sequence Y comprises multiple layers. Nonetheless the lateral variation in the wavelet of Reflector 7 is suggestive of a sequence of thin layers of which all or part, coinciding with the décollement fault zone, may be sheared as described by drill hole and field studies [*Fagereng*, 2011; *Kimura et al.*, 2012; *Rowe et al.*, 2013].

3.1.2. SSZ Low-Impedance Layer

A ∼1.5 km thick zone of low V_p (LVZ) appears to extend from sequence Y to the top of the Hikurangi Plateau (Reflector 8). Velocities decrease updip from ∼5 km/s at 10 km depth to ∼3 km/s at 6 km depth (Figures 2b, 3b, and 3c). Relative to overlying interval velocities, the LVZ represents a velocity inversion of 400–600 m/s. The lower boundary of the LVZ coincides with a positive-polarity unconformity at which horizontally stratified layers, with high frequency content, onlap highly reflective and inclined (∼7° dip) strata characterized by a lower frequency content (Figure 3a). We interpret this unconformity as Reflector 8 and a boundary between marine basin-floor sediments of Early and Late Cretaceous age (MES of *Davy et al.* [2008]) deposited on a succession of intercalated volcanic rocks, volcaniclastics and sediment of the Hikurangi Plateau (HKB of *Davy et al.* [2008]). One-dimensional waveform modeling indicates low seismic impedance for the SSZ which we attribute to under consolidated, overpressured sediment beneath the décollement. The presence of an oceanic seamount piercing through the sediments is inferred based on pinch out of well stratified HKB sediments against a zone of chaotic seismic character and the appearance of low-velocity zones (LVZs) bounding the top of the chaotic seismic body (Figures 2b and 3).

Reflector 7 can be traced westward downdip to a depth of ∼9 km, at km 50 (Figure 4a). Farther west, however, the continuity of the SSZ is disrupted. Relying on the location of dipping diffracted energy associated with fault planes we interpret a 4 km step down in the décollement from Reflector 7 to Reflector 8 at ∼12 km depth. This deeper décollement level corresponds to the plate boundary west of Porangahau Ridge and below the inner wedge of the accretionary prism. Given the absence of a clear interface reflection under the inner wedge, an uncertainty of ∼10% in our velocity model is introducing a potentially considerable error in the depth of the plate interface at this location. For example, the plate boundary identified in Figure 2 is 2 km deeper than the margin wide boundary constructed by combining regional earthquake and seismic reflection data [*Williams et al.*, 2013]. However, the two surfaces are in agreement at the western end of 05CM-38 and beneath Porangahau Ridge.

3.2. Splay Faults

The seismic transect reveals three main thrust fault clusters and ridges in the overriding plate (Figures 1 and 2). Bathymetric data reveal the Porangahau and Akito Ridges as prominent outer accretionary wedge highs that are continuous for over 100 km along strike (Figure 1). These ridges have been previously described at a regional scale based on seismic interpretation of a wide range of seismic profiles across and along the Hikurangi margin [*Barker et al.*, 2009; *Ghisetti et al.*, 2016; *Lewis and Pettinga*, 1993]. The PSDM version of profile 05CM-38 shows the relationship of the major upper plate splay faults to the décollement. The deformation front and zones of proto-thrusts are imaged on an adjoining seismic line, SO191-4, 15 km seaward of Akito Ridge [*Barnes et al.*, 2010; *Ghisetti et al.*, 2016]. A lateral change in the pattern of thrusting on this part of the margin can be observed in terms of dip angle, fault extension, and geometry of each thrust fault cluster (Figure 2). The easternmost group of faults, beneath Akito ridge (CDP 600-1700), is characterized by ∼6.5–7.5 km long thrust faults dipping up to ∼30-35° that offset the Miocene to Pleistocene sequence (reflections 4 and 5B). Their clear splay fault branching, from the décollement at ∼8 km depth, delineates the subduction interface at this location (Figure 2).
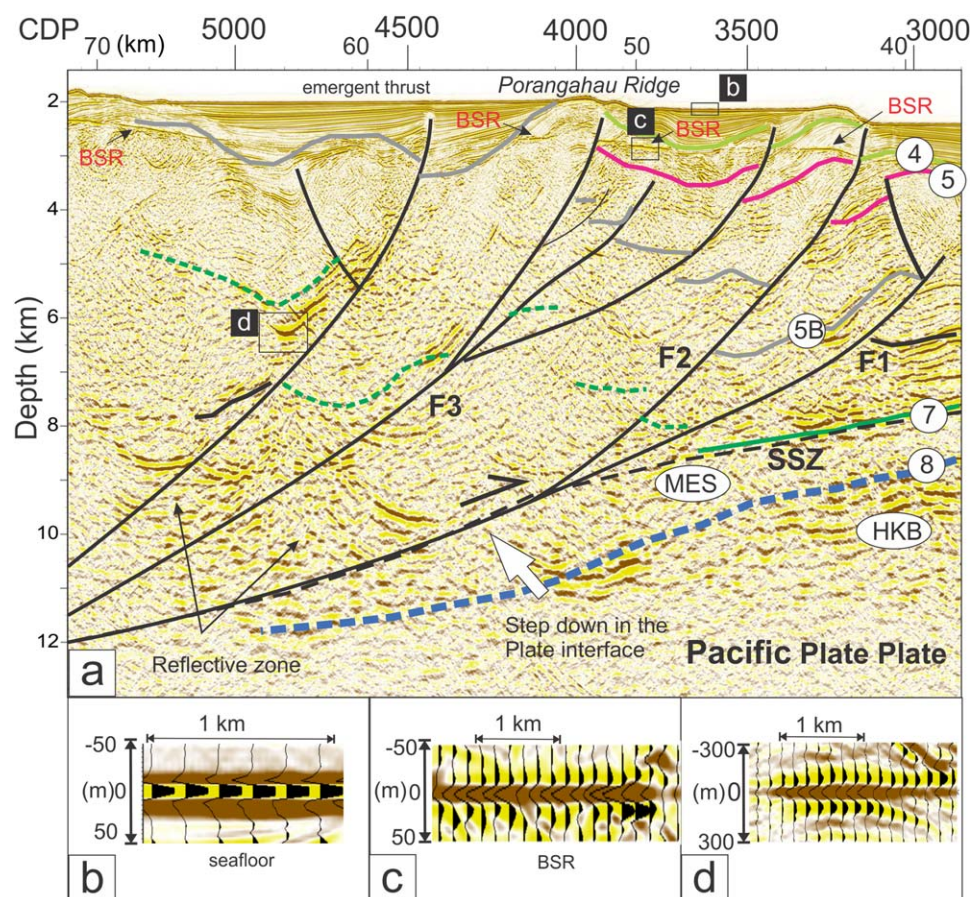
Figure 4. (a) Enlarged seismic image, between CDP 2890 and 5500 (km 38–71), showing a set of faults associated with a major splay fault (labeled F1, F2, and F3) in the region of Porangahau Ridge. Interpreted faults and seismic reflections are from Figure 2. MES, Mesozoic sequence and HKB, Hikurangi basement. We interpret a step down in the décollement from Reflector 7 to Reflector 8 potentially coinciding with the plate boundary. Plots (b) and (c) show the polarity of seismic traces along the seafloor and along the bottom-simulating reflector (BSR), respectively. Plot (d) shows the polarity of the reflection at a zone of high reflectivity, interpreted to be a zone of fluid accumulation beneath Porangahau Ridge.

Further west, Porangahau Ridge is characterized by three semicontinuous west-dipping splay-faults (F1, F2, and F3 in Figure 4) that appear to branch upward from where the dip of the plate boundary interface increases (CDP 3000–5000 and km 40–65). Prominent fault planes ramp and steepen from dips of 20° to greater than 60° approaching the seafloor. Splay fault planes have bright reflections associated, sometimes with polarity comparable to BSRs (i.e., reverse polarity with respect to the seafloor; Figures 4b–4d) and reminiscent of splay faults branching from the décollement at the Nankai subduction zone, southeast Japan [*Bangs et al.*, 2009].

The easternmost splay fault, F1, is associated with a blind thrust (Figure 4a). Porangahau Ridge, results from deformation along a second splay fault, F3, soling from the décollement at ~12 km depth (Figures 2 and 4a) and additional thrust faults branching at depths of 5–7 km. A third splay fault, F2, merges with the décollement near the step down at CDP 4000, >50 km from the deformation front (Figure 4a). We are not able to confidently trace coherent crustal seismic reflections beneath Porangahau Ridge on the final PSDM image but footwall and hanging-wall cut-offs are interpretable in places and imply that Reflector 7 and SSZ sediments step up along the major splay faults consistent with faster midcrust velocities ($V_p > 4.5$ km/s) between km 55 and 70 (Figure 2b). In places, imbricated SSZ sediment appears as highly reflective energy (Figure 4a).

A zone of homogeneous seismic reflectivity separates the Porangahau region from the next landward ridge (between CDP 7300–9000 and km 95–115) indicating steep dips or uniform rocks with no contrasts in acoustic impedance. One main splay fault branches from the décollement dipping 10–20° at 14 km depth
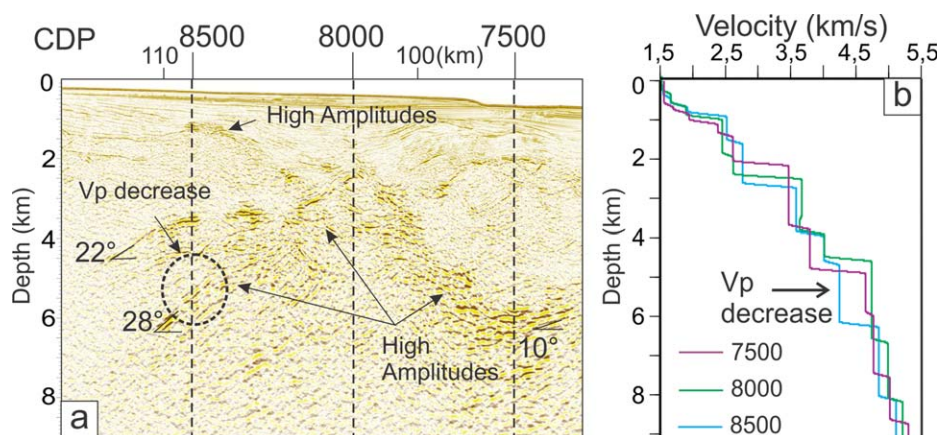
Figure 5. (a) Enlarged seismic image, between CDP 7630 and 8900 (km 93–114) showing dipping (up to 28°) bright reflections at the high amplitude wedge interpreted to be underplated material or 100–110 Ma Torlesse terrane accretionary rocks. (b) *P* wave velocity (V_p) at the location of three CDPs (7500, 8000, and 8500) within the high amplitude wedge. A relative lateral velocity decrease, documented by CDP 8500 at ∼5 km depth, indicates preferential zones for fluid accumulations.

(Figure 2) and steepens to >60° beneath the southern continuation of Paoanui Ridge (CDP 6000). To the west, the depth extent of thrust faults becomes less clear, while entering a zone marked by a distinct reflectivity (Figures 2a and 5).

3.3. High Amplitude Wedge

Thrust faults west of Porangahau Ridge (CDP 7300–9000) are rooted in a zone of high velocities (>4.8 km/s). These faults surround a high-amplitude reflectivity wedge ∼25 km wide and ∼7 km thick above the décollement (Figures 2 and 5). This high amplitude wedge has been previously described from time migrated seismic data and suggested to be a "backstop" to the outer wedge [*Barker et al.*, 2009]. In the depth-migrated profile amplitudes are strongest toward the shallowest part of the wedge and bright reflections are in distinct packages resembling the seismic character of the SSZ, further east, where the LVZs coincide with bright-well stratified reflectors (Figures (2 and 3), and 5) interpreted as Cretaceous age sediments [*Bland et al.*, 2015]. Several layers, 1–2 km thick, delimited by upper and lower bright reflections, with internal weak reflectivity zones, are stacked at variable dips (10–30°) (Figure 5). We outline two plausible interpretations of these reflective packages:

1. Due to the resemblance of the reflective packages to the MES sediments, it is possible that these structures are duplexes of fluid-rich underplated MES sediments. If this is correct, the core of the underplated imbricate slices will be mainly Cretaceous and Paleogene (SSZ) strata emplaced by northwest dipping thrust sheets, that continue over 100 km northward along strike [*Barker et al.*, 2009] to where rocks of this age are exposed as an inlier on Mahia Peninsula [*Field et al.*, 1997] and in southern Hawkes Bay [*Pettinga*, 1982]. A zone, experiencing a lateral V_p decrease, is also seen in the velocity analysis for discrete CDP gathers at the westernmost inferred underplated duplex (Figure 5). High amplitude reflections sitting above the zone of decreased V_p (Figure 5a) may indicate focused fluid migration upward from compacting underplated and imbricated rocks. This model would require a large proportion of the offshore forearc to be composed of underplated sediments, which may be implausible. If the large reflective package at the landward side of 05CM-38 is indeed underplated sediment, it would have been underplated beneath a very thin forearc (∼2 km thick), or involve large uplift and erosion of the forearc to accommodate the underplating.
2. It is also possible that this wedge of high amplitude reflections beneath offshore Wairarapa and Hawke Bay constitutes 100–110 Ma accretionary margin rocks equivalent to deformed Torlesse composite terrane accretionary rocks of this age exposed onshore [*Bland et al.*, 2015; *Mountjoy and Barnes*, 2011]. If this is the case, the imbricated high-amplitude zone is equivalent to the frontal sequence of the inactive Mesozoic accretionary wedge under the northern Chatham Rise [*Barnes et al.*, 2010]. The overall higher V_p observed in this reflective unit (>5 km/s) may be more consistent with this hypothesis than the underplating hypothesis.

Overlying the highly reflective section described here are Miocene to recent shelf and slope basin sediments, which are up to ~3 km thick beneath the upper margin (Figure 5) and generally thin seaward [*Barnes et al.*, 2010]. Tawatawa-1 well, at the western end of 05CM-38 (Figure 2), reached 1560 m and penetrated the basal part of Late Miocene sediments [*Field et al.*, 1997]. The sequences of the upper margin are exposed in uplifted forearc basins on land and basin fill architecture is strongly influenced by active tectonics expressed by regionally extensive unconformities and normal faulting (Figure 2).

4. Discussion

4.1. Plate Interface, Subducting Sediment, and Fluid Distribution

The eastern end of seismic line, 05CM-38, images the trench slope and active plate décollement at 7 km deep (Figure 2). Here the décollement coincides with the upper part of a unit inferred by *Barnes et al.* [2010] to comprise a condensed sequence of strongly reflective Late Cretaceous-Early Oligocene (70–32 Ma) marine nannofossil chalks, mudstones, and chert and referred to in previous work east of the trench as sequence Y (Seq Y in Figures 2 and 6a) [*Davy et al.*, 2008]. Beneath the décollement, up to 1.5 km thick sequence of Mesozoic sediments is being subducted along the Hikurangi margin beneath the active plate boundary thrust dipping ~2° landward (Figures 2 and 6a, MES of *Davy et al.* [2008]). Our velocity analysis reveal that the MES sequence, coinciding with what we describe as the subducted sedimentary zone (SSZ), is associated with >10 km long zones of anomalously low V_p (LVZs in Figure 2b). The same association between sequence Y, underlying fluid-rich MES sediments and anomalous low velocities persists further south, in Pegasus Basin, where the LVZ is up to 3 km thick at 8 km depth [*Plaza-Faverola et al.*, 2012] and is interpreted to extend beneath the North Island before stepping down to the top of the Hikurangi Plateau [*Bassett et al.*, 2014].

The occurrence of an LVZ within the SSZ is broadly interpreted as indication of undercompaction induced by the presence of pore-filling fluids commonly trapped within subducting sediments that are rapidly buried [e.g., *Bangs et al.*, 2009, 1990; *Calahorrano et al.*, 2008; *Collot et al.*, 1996; *Kamei et al.*, 2012; *Kitajima and*
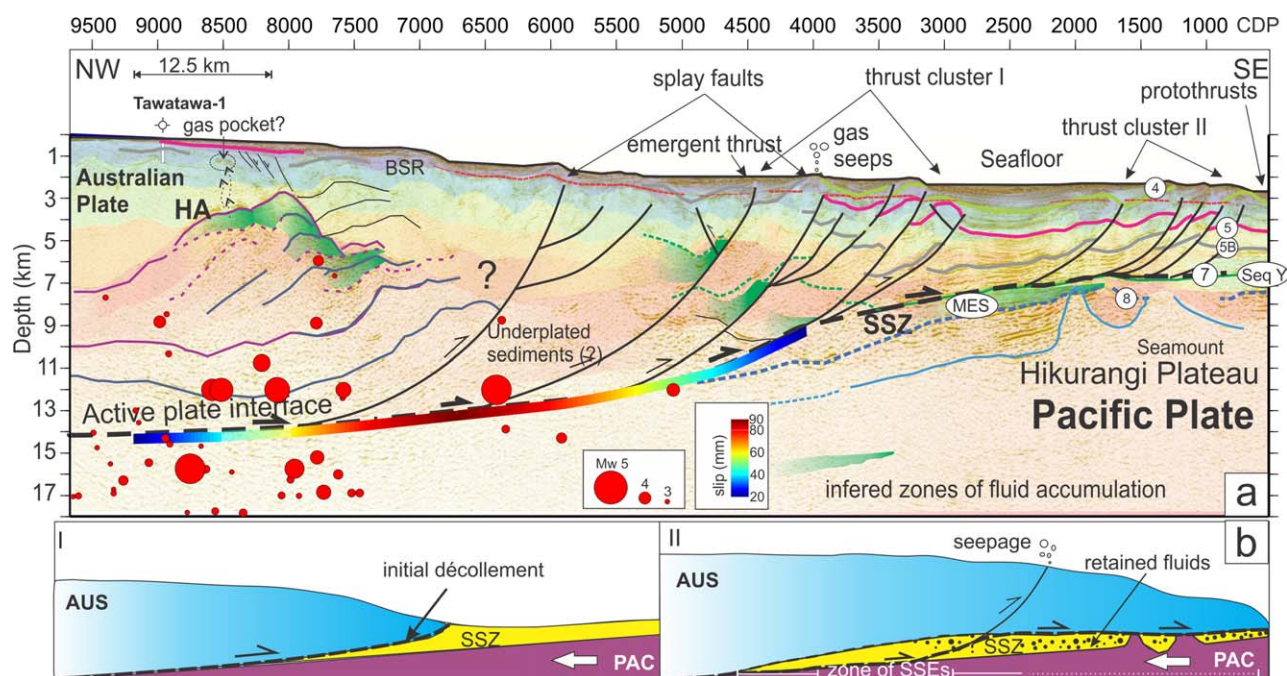

Figure 6. (a) Integrated prestack depth-migrated seismic transect along profile 05CM-38 superimposed on the *P* wave velocity model. Interpreted faults and seismic reflections are from Figure 2. Red filled circles are hypocenters of earthquakes, plotted in Figure 1, which occurred within a 50 km along strike section of 05CM-38. Cumulative slip in the 2011 East Coast slow slip event (SSE) sequence from *Wallace et al.* [2012] on the plate interface (rainbow colors, see scale bar). HA, high amplitude wedge and MES, Mesozoic sequence. Our interpretation maintains there is a link between slow slip, sediment underplating, and splay fault branching from the subduction interface along this part of the margin. Preferential zones of fluid accumulation are expected to be primarily related to sediments in the subducted sediment zone (SSZ). Vertical exaggeration is 2:1. (b) Schematic representation of the development of splay faults, the step down in the décollement and associated fluid migration. AUS, Australian Plate; PAC, Pacific Plate; and SSE, slow slip event.

Saffer, 2012; *Vannucchi et al.*, 2012]. Further to the north, along the northern Hikurangi margin, a thermomechanical-fluid model predicts that significant overpressures, with fluid pressure ratios of 0.95 or higher, may develop along the subduction interface at ∼8–9 km depth, landward of a subducting seamount, if a thin, low-permeability (10^{-k} m^2) seal is present along the décollement [*Ellis et al.*, 2015]. Our reflectivity modeling of Reflector 7, coinciding with the décollement and the top of sequence Y, reveals this boundary to be a thin high-velocity layer (3.9 km/s) of positive-polarity reflection coefficient and approximately 100 m thick (Figure 3h). The presence of a seamount beneath the Akito Ridge and a sealing sequence Y, provide an ideal setting for the generation of significant overpressures, necessary to explain the LVZs documented to both sides of the interpreted seamount on line 05CM-38 (Figure 2).

With respect to overlying interval velocities, the magnitude of the V_p inversion varies within the LVZ, increasing from 400 km/s at the downdip end to 600 km/s toward the updip end (Figures 3b and 3c). Structurally, a zone within 40 km of the trench is likely to be the preferred location for accumulation of fluids, migrating updip along the SSZ and accompanied by sediment compaction downdip (Figure 6b). This is similar to the settings of Muroto transect, Nankai [*Bangs et al.*, 2009], and the Ecuador margin [*Calahorrano et al.*, 2008], which document a trend of decreasing V_p, increasing porosity, decreasing effective stress, and increasing pore pressure ratio toward the trench. Our results suggest thus that the central Hikurangi margin is characterized by a mechanically weak plate interface in the outer wedge, consistent with the low critical wedge taper there [*Fagereng*, 2011]. Speculatively, the decrease in V_p within the SSZ >40 km away from the deformation front may be the result of sediment compaction leading to increasing shear stress resulting in down-stepping of the décollement to ∼12 km depth that represents a transfer of slip to the oceanic crust beneath Porangahau Ridge.

Beneath Porangahau Ridge the 8 km ramp structure coincides with a 20° increase in dip of the décollement and where west-dipping splay faults converge. The sediments above the décollement appear imbricated between splay faults (Figure 4) resulting in a complex seismic structure. These imbricated sediments, similar to the high amplitude wedge to the west, could be interpreted as a complex zone of underplating and duplex structures, or as 100–110 Ma accretionary margin Torlesse terrane rocks. In either case, the step down floor thrust (Figures 2 and 6) may account for thickening in the overriding plate and may accommodate interplate shortening [e.g., *Nicol and Beavan*, 2003]. If there is any shortening, represented by underplating, it may represent a component of the unaccounted margin-perpendicular shortening on this part of the Hikurangi margin in the last 2 Myr [*Ghisetti et al.*, 2016].

The SSZ loses coherency beneath the imbricated sediments and the PSDM velocity analysis does not resolve the presence of low V_p. Although a similar pattern of an SSZ with excess pore-fluid pressures toward the trench is documented from PSDM across the southern Hikurangi margin [*Plaza-Faverola et al.*, 2012], we cannot entirely rule out the possibility of overpressure zones deeper along the décollement. Nonetheless, the sediments above the décollement and beneath Porangahau Ridge (Figures 2a and 4), are highly reflective and show reverse polarity reflections, with variable dip, along segments that terminate at major splay faults (Figure 4). Higher V_p (4.5–5.0 km/s at 5–8 km depth) in this region above the décollement, lead us to believe that sediments here are significantly indurated and subjected to high stress perhaps facilitating fluid migration toward more permeable splay faults (Figure 6). Zones of high stress are prone to extensive fracturing and constant reopening of conduits for fluids [*Curewitz and Karson*, 1997; *Sibson*, 1994]. Fault intersections and linkage of fault segments favor fluid migration and redistribution [*Curewitz and Karson*, 1997]. We suggest that down-stepping of the décollement together with splay fault branching provides an ideal setting for fluid migration from the SSZ toward the surface, explaining documented perturbation of the gas hydrate stability zone [*Pecher et al.*, 2010; *Crutchley et al.*, 2011] and seafloor seepage at Porangahau Ridge [*Bialas*, 2011]. Seafloor seepage induced by fluid migration along faults is a transient process that may occur in pulses. In active faulting settings, such periodicity is believed to be tied to stress cycles through creation or reduction of permeability [*Fisher et al.*, 1995; *Sibson*, 2013] and where periodic cracking and sealing of microstructures can take place in less than 10 days [*Fisher and Brantley*, 2014], similar to the duration of short-term (1–3 weeks) SSEs. Furthermore, similar seismic observations (i.e., high amplitude-reverse polarity reflections, associated with major thrust faults) are indicative of permeable faults playing a key role in the transport of fluids from subducting sediments toward the seafloor [e.g., *Bangs et al.*, 1999; *Ranero et al.*, 2008; *Shipley et al.*, 1994].

4.2. Relationship to Slow Slip

The relationship between our seismic observations and geodetic data are summarized in Figure 6a where we compare the PSDM seismic image with the distribution of slip during the slow slip event in June/July 2011 that was recorded by shore-based continuous GPS stations [*Wallace et al.*, 2012]. The zone of maximum cumulative slip (i.e., up to 90 mm), correlates with the zone of splay fault branching at the lowermost level of the décollement (~14 km depth), west of the plate interface thrust ramp (Figure 6a). However, we emphasize that the detailed slow slip distribution beneath the offshore region that is based on land-based GPS data, is not well-constrained, particularly the location of the updip limit of slow slip. For example, *Wallace et al.* [2016] recently showed from a seafloor geodetic experiment that the offshore slow slip further north along the Hikurangi margin extends closer to the trench than inferred from GPS data alone.

Many slow slip source areas at circum-Pacific subduction zones are associated with low-velocity zones, such as Mexico [*Song et al.*, 2009], Cascadia [*Audet et al.*, 2009], and southwest Japan [*Kamei et al.*, 2012; *Kitajima and Saffer*, 2012; *Kodaira et al.*, 2004]. These low-velocity zones are thought to represent fluid-rich material at the plate interface. This association between slow slip (and related seismic phenomena) and low-velocity zones has contributed to the widely held view that SSEs are promoted by high fluid pressures. Although the slow slip events observed in the Porangahau region appear to terminate just landward of the LVZs that we observe on 05CM-38 (Figures 2b and 6a), it is certainly plausible that these SSEs such as that in 2011 actually continue through the LVZ all the way to the trench, similar to what is observed offshore the northern Hikurangi margin [*Wallace et al.*, 2016]. Seafloor geodetic experiments should be undertaken in this region to determine the distribution of SSE slip with respect to the LVZ observed in 05CM-38.

Seismic velocities near the plate interface in the SSE zone on 05CM-38 appears to be relatively high (Figures 2b and 6a). *Bassett et al.* [2014] made a similar observation of higher wave speeds along 05CM-38 compared to portions of the forearc further north. As discussed in section 4.1, our result of higher velocities (Figure 2b) could be either real or due to difficulties in picking reflections for the semblance analysis in this part of the margin (supporting information Figure S1.1). On the basis that these higher velocities are resolvable, our results suggest a lack of widespread high fluid pressure within the main portion of the geodetically determined SSE zone. This is in distinct contrast to what has been observed in other slow slip regions, where fluids are thought to be abundant.

To date, most theoretical and observational studies suggest that SSEs are a consequence of transitional fault zone stability, which can be influenced by excess fluid pressures [*Kodaira et al.*, 2004; *Liu and Rice*, 2005], transitional frictional properties [*Scholz and Campos*, 2012], fault rigidity [*Leeman et al.*, 2016], or some combination of all three [*Saffer and Wallace*, 2015]. If SSEs observed offshore northern Wairarapa are not clearly associated with excess fluid pressure, it is possible that the properties of the rocks in the fault zone (friction, rigidity) play a larger role, or that other factors may be involved. Numerical modeling studies have also shown that spatial heterogeneity of fault frictional properties and/or rheology can widen the conditions required for SSE behavior [*Ando et al.*, 2012; *Lavier et al.*, 2013; *Skarbek et al.*, 2012], which agrees well with outcrop observations of exhumed subduction complexes where SSE-like processes are inferred [*Fagereng and Sibson*, 2010]. Most areas that host shallow SSEs (e.g., <15 km depth) also coincide with rough subducting seafloor, further suggesting that heterogeneity of plate boundary structure and properties may help to promote shallow SSEs [*Saffer and Wallace*, 2015; *Wang and Bilek*, 2014]. Our analysis of 05CM-38 does suggest significant heterogeneity of plate boundary properties exists there, including: LVZs alternating with subducted seamounts, step-down of the décollement to different stratigraphic levels, and numerous branching splay faults (Figure 6). Together, these factors could produce significant spatial variation in frictional properties of the plate interface and help to promote the recorded SSEs.

To explain the observation of the 2011 East Coast SSE sequence offshore northern Wairarapa, in a region of the plate interface that is otherwise partially (~75%) coupled, *Wallace et al.* [2012] proposed that the transition zone between interseismic locking (south) and aseismic creep (north) may be a region characterized by highly heterogeneous plate interface properties. That is, a patchwork of asperities that are strongly velocity weakening (i.e., slip in earthquakes), surrounded by regions of the subduction thrust fault with transitional frictional properties that undergo episodic slow slip. Indeed, seismicity, that accompanied the 2011 SSE sequence, cluster on the western downdip edge of the cumulative slip distribution (Figures 1b and 6a) and moment tensor solutions of two of the largest events indicate thrust faulting, with a small component of

strike-slip motion [*Wallace et al.*, 2012]. To test the degree to which high fluid pressures play a role in offshore Wairarapa SSEs and locking versus other processes (for example, fault rock properties, heterogeneity), additional experiments such as offshore magnetotelluric observations and OBS deployments are required.

Finally, we speculate that seafloor seepage at Porangahau Ridge [*Bialas*, 2011] may occur episodically in response to stress changes at the décollement and overlying imbricated sediments during SSEs. The maximum rates of slow slip are distributed at the zone where major splay faults branch out from the décollement (Figure 6a). We suggest that a redistribution of stress and hence fluid pressure post-SSE may induce pulses of fluid release, as an analogous mechanism to postseismic discharge of fluids [*Sibson*, 1994]. Enhanced fluid flow during slow slip has been observed previously using seafloor monitoring systems offshore Costa Rica [*Brown et al.*, 2005; *Davis and Villinger*, 2006; *Solomon et al.*, 2009]. This hypothesis is consistent with one-dimensional models of fluid expulsion at the Porangahau Ridge, which indicates inferred doming of the base of gas hydrate stability by advective heat flow, at realistic fluid-flow rates, can be explained by fluids sourced at depth, possibly from the region of the décollement [*Barnes et al.*, 2010]. If warm fluids from deep within a subduction system are transported sufficiently rapidly upward along permeable splay faults toward the gas hydrate system and the seafloor, they can promote the dissociation of gas hydrates [*Crutchley et al.*, 2014] and potentially provide a window into processes occurring on the subduction interface [*Lauer and Saffer*, 2015]. Testing this hypothesis requires temporal data on SEEs together with observations of fluid flux rates.

5. Conclusions

We have undertaken prestack depth migration of line 05CM-38 across the central Hikurangi subduction thrust that experienced a short duration slow-lip in 2011, and transects the accretionary margin that is in the transition zone between interseismic locking and aseismic creep. The results summarized in Figure 6 show that:

1. The active plate décollement, up to 50 km from the deformation front, coincides with a low-permeability condensed sequence of strongly reflective Late Cretaceous-Early Oligocene marine nannofossil chalks. Beneath the décollement, up to 1.5 km of low velocity sequences constitute a subduction sedimentary zone interpreted as undercompacted, induced by the presense of pore-filling fluids, and providing an explanation for a mechanically weak low critical wedge taper along this part of the Hikurangi margin.
2. We regard the downdip trend of increasing V_p, decreasing porosity and increasing shear stress at distances greater than 40 km away from the deformation front may be responsible for the down-stepping of the décollement from 8 to ~12 km depth. The down-stepping fault represents a transfer of slip to the oceanic crust beneath Porangahau Ridge, possibly driving underplating along the megathrust décollement. The down-stepping ramp merges with prominent landward dipping splay thrust faults that extend from the décollement to the seafloor, providing pathways for fluid migration toward the surface and explaining documented perturbation of the gas hydrate stability zone and seafloor seepage at Porangahau Ridge.
3. A highly reflective zone in the wedge, west of Porangahau Ridge and beneath the shelf, can be interpreted as either (a) a region of sediment underplating or (b) Torlesse terrane that was accreted during a much earlier phase of subduction. The highly reflective part of the forearc and splay fault branching overlies the portion of the interface that undergoes large slow slip. To resolve the physical controls on shallow SSEs beneath Porangahau, it is necessary to better understand whether or not excess pore-fluid pressures are present at the plate interface in this region. If the high V_p of this part of the forearc and interface is real, then it might suggest that other factors such as fault rock properties and plate boundary heterogeneity are more important in this area.

References

Ando, R., N. Takeda, and T. Yamashita (2012), Propagation dynamics of seismic and aseismic slip governed by fault heterogeneity and Newtonian rheology, *J. Geophys. Res.*, *117*, B11308, doi:10.1029/2012JB009532.

Audet, P. (2010), Temporal variations in crustal scattering structure near Parkfield, California, using receiver functions, *Bull. Seismol. Soc. Am.*, *100*(3), 1356–1362, doi:10.1785/0120090299.

Audet, P., M. G. Bostock, N. I. Christensen, and S. M. Peacock (2009), Seismic evidence for overpressured subducted oceanic crust and megathrust fault sealing, *Nature*, *457*(7225), 76–78.

Bangs, N. L. B., G. K. Westbrook, J. W. Ladd, and P. Buhl (1990), Seismic velocities from the Barbados Ridge complex: Indicators of high pore fluid pressures in an accretionary complex, *J. Geophys. Res.*, *95*(B6), 8767–8782.

Bangs, N. L. B., T. H. Shipley, J. C. Moore, and G. F. Moore (1999), Fluid accumulation and channeling along the northern Barbados Ridge decollement thrust, *J. Geophys. Res.*, *104*(B9), 20,399–20,414.

Bangs, N. L. B., G. F. Moore, S. P. S. Gulick, E. M. Pangborn, H. J. Tobin, S. Kuramoto, and A. Taira (2009), Broad, weak regions of the Nankai Megathrust and implications for shallow coseismic slip, *Earth Planet. Sci. Lett.*, *284*(1), 44–49.

Barker, D. H. N., R. Sutherland, S. Henrys, and S. Bannister (2009), Geometry of the Hikurangi subduction thrust and upper plate, North Island, New Zealand, *Geochem. Geophys. Geosyst.*, *10*, Q02007, doi:10.1029/2008GC002153.

Barnes, P. M., and B. Mercier de Lepinay (1997), Rates and mechanics of rapid frontal accretion along the very obliquely convergent southern Hikurangi margin, New Zealand, *J. Geophys. Res.*, *102*(B11), 24,931–24,952.

Barnes, P. M., G. Lamarche, J. Bialas, S. Henrys, I. Pecher, G. L. Netzeband, J. Greinert, J. J. Mountjoy, K. Pedley, and G. Crutchley (2010), Tectonic and geological framework for gas hydrates and cold seeps on the Hikurangi subduction margin, New Zealand, *Mar. Geol.*, *272*(1), 26–48.

Bartlow, N. M., L. M. Wallace, R. J. Beavan, S. Bannister, and P. Segall (2014), Time-dependent modeling of slow slip events and associated seismicity and tremor at the Hikurangi subduction zone, New Zealand, *J. Geophys. Res. Solid Earth*, *119*, 734–753, doi:10.1002/2013JB010609.

Bassett, D., R. Sutherland, and S. Henrys (2014), Slow wavespeeds and fluid overpressure in a region of shallow geodetic locking and slow slip, Hikurangi subduction margin, New Zealand, *Earth Planet. Sci. Lett.*, *389*, 1–13, doi:10.1016/j.epsl.2013.12.021.

Bell, R., R. Sutherland, D. H. N. Barker, S. Henrys, S. Bannister, L. Wallace, and J. Beavan (2010), Seismic reflection character of the Hikurangi subduction interface, New Zealand, in the region of repeated Gisborne slow slip events, *Geophys. J. Int.*, *180*(1), 34–48.

Berndt, C. (2005), Focused fluid flow in passive continental margins, *Philos. Trans. R. Soc. A*, *363*(1837), 2855–2871, doi:10.1098/rsta.2005.1666.

Bialas, J. (2011), FS SONNE Fahrtbericht/Cruise Report SO-214 NEMESYS 09.03.−05.04.2011 Wellington - Wellington, 06. - 22.04.2011 Wellington – Auckland, *Rep.*, 174 pp, IFM-GEOMAR, Kiel.

Bland, K. J., C. I. Uruski, and M. J. Isaac (2015), Pegasus Basin, eastern New Zealand: A stratigraphic record of subsidence and subduction, ancient and modern, *N. Z. J. Geol. Geophys.*, *58*(4), 319–343.

Bolton, A., and A. Maltman (1998), Fluid-flow pathways in actively deforming sediments: The role of pore fluid pressures and volume change, *Mar. Pet. Geol.*, *15*(4), 281–297.

Brown, K. M., M. D. Tryon, H. R. DeShon, L. M. Dorman, and S. Y. Schwartz (2005), Correlated transient fluid pulsing and seismic tremor in the Costa Rica subduction zone, *Earth Planet. Sci. Lett.*, *238*(1), 189–203.

Bugge, T., S. Befring, R. H. Belderson, T. Eidvin, E. Jansen, N. H. Kenyon, H. Holtedahl, and H. P. Sejrup (1987), A giant three-stage submarine slide off Norway, *Geo Mar. Lett.*, *7*(4), 191–198.

Calahorrano, B. A., V. Sallarès, J. Y. Collot, F. Sage, and C. R. Ranero (2008), Nonlinear variations of the physical properties along the southern Ecuador subduction channel: Results from depth-migrated seismic data, *Earth Planet. Sci. Lett.*, *267*(3–4), 453–467.

Collot, J. Y., J. Delteil, K. B. Lewis, B. Davy, G. Lamarche, J. C. Audru, P. Barnes, F. Chanier, E. Chaumillon, and S. Lallemand (1996), From oblique subduction to intra-continental transpression: Structures of the southern Kermadec-Hikurangi margin from multibeam bathymetry, side-scan sonar and seismic reflection, *Mar. Geophys. Res.*, *18*, 357–381.

Crutchley, G. J., A. R. Gorman, I. A. Pecher, S. Toulmin, and S. A. Henrys (2011), Geological controls on focused fluid flow through the gas hydrate stability zone on the southern Hikurangi Margin of New Zealand, evidenced from multi-channel seismic data, *Mar. Pet. Geol.*, *28*, 1915–1931.

Crutchley, G., D. Klaeschen, L. Planert, J. Bialas, C. Berndt, C. Papenberg, C. Hensen, M. Hornbach, S. Krastel, and W. Brückmann (2014), The impact of fluid advection on gas hydrate stability: Investigations at sites of methane seepage offshore Costa Rica, *Earth Planet. Sci. Lett.*, *401*, 95–109, doi:10.1016/j.epsl.2014.05.045.

Curewitz, D., and J. A. Karson (1997), Structural settings of hydrothermal outflow: Fracture permeability maintained by fault propagation and interaction, *J. Volcanol. Geotherm. Res.*, *79*(3), 149–168.

Davey, F. J., M. Hampton, J. Childs, M. A. Fisher, K. Lewis, and J. R. Pettinga (1986), Structure of a growing accretionary prism, Hikurangi margin, New Zealand, *Geology*, *14*, 663–666.

Davis, E., M. Heesemann, and K. Wang (2011), Evidence for episodic aseismic slip across the subduction seismogenic zone off Costa Rica: CORK borehole pressure observations at the subduction prism toe, *Earth Planet. Sci. Lett.*, *306*(3), 299–305.

Davis, E. E., and H. W. Villinger (2006), Transient formation fluid pressures and temperatures in the Costa Rica forearc prism and subducting oceanic basement: CORK monitoring at ODP Sites 1253 and 1255, *Earth Planet. Sci. Lett.*, *245*, 232–244.

Davy, B., K. Hoernle, and R. Werner (2008), Hikurangi Plateau: Crustal structure, rifted formation, and Gondwana subduction history, *Geochem. Geophys. Geosyst.*, *9*, Q07004, doi:10.1029/2007GC001855.

Ellis, S., Å. Fagereng, D. Barker, S. Henrys, D. Saffer, L. Wallace, C. Williams, and R. Harris (2015), Fluid budgets along the northern Hikurangi subduction margin, New Zealand: The effect of a subducting seamount on fluid pressure, *Geophys. J. Int.*, *202*(1), 277–297, doi:10.1093/gji/ggv127.

Etiope, G. (2009), Natural emissions of methane from geological seepage in Europe, *Atmos. Environ.*, *43*(7), 1430–1443.

Fagereng, Å. (2011), Geology of the seismogenic subduction thrust interface, *Geol. Soc. Spec. Publ.*, *359*(1), 55–76, doi:10.1144/sp359.4.

Fagereng, Å., and R. H. Sibson (2010), Melange rheology and seismic style, *Geology*, *38*, 751–754.

Field, B. D., et al. (1997), Cretaceous-Cenozoic geology and petroleum systems of the east coast region, New Zealand, *Inst. Geol. Nucl. Sci. Geol. Monogr.*, *19*, 301.

Fisher, D. M., and S. L. Brantley (2014), The role of silica redistribution in the evolution of slip instabilities along subduction interfaces: Constraints from the Kodiak accretionary complex, Alaska, *J. Struct. Geol.*, *69*, 395–414.

Fisher, D. M., S. L. Brantley, M. Everett, and J. Dzvonik (1995), Cyclic fluid flow through a regionally extensive fracture network within the Kodiak accretionary prism, *J. Geophys. Res.*, *100*(B7), 12,881–12,894.

Gay, A., M. Lopez, P. Cochonat, N. Sultan, E. Cauquil, and F. Brigaud (2003), Sinuous pockmark belt as indicator of a shallow buried turbiditic channel on the lower slope of the Congo Basin, West African Margin, *Geol. Soc. Spec. Publ.*, *216*(1), 173–189.

Ghisetti, F., P. Barnes, S. Ellis, A. Plaza-Faverola, and D. H. N. Barker (2016), The last 2 Myr of accretionary wedge construction in the central Hikurangi margin (North Island, New Zealand): Insights from structural modeling, *Geochem. Geophys. Geosyst.*, *17*, 2661–2686, doi:10.1002/2016GC006341.

Hoffmann, H.-J., and T. Reston (1992), Nature of the S reflector beneath the Galicia Banks rifted margin: Preliminary results from prestack depth migration, *Geology*, *20*(12), 1091–1094.

Hovland, M., R. Heggland, M. H. de Vries, and T. I. Tjelta (2010), Unit-pockmarks and their potential significance for predicting fluid flow, *Mar. Pet. Geol.*, *27*, 1190–1199.

Ito, A., G. Fujie, S. Miura, K. Kodaira, and Y. Kaneda (2005), Bending of the subducting oceanic plate and its implications for rupture propagation of large interplate earthquakes off Miyagi Japan, in the Japan Trench subduction zones, *Geophys. Res. Lett.*, *32*, L05310, doi: 10.01029/02004GL022307.

Judd, A. G., and M. Hovland (2007), *Seabed Fluid Flow: The Impact of Geology, Biology and the Marine Environment*, 475 pp., Cambridge Univ. Press, Cambridge, U. K.

Kamei, R., R. G. Pratt, and T. Tsuji (2012), Waveform tomography imaging of a megasplay fault system in the seismogenic Nankai subduction zone, *Earth Planet. Sci. Lett.*, *317*, 343–353, doi:10.1016/j.epsl.2011.10.042.

Kimura, G., A. Yamaguchi, M. Hojo, Y. Kitamura, J. Kameda, K. Ujiie, Y. Hamada, M. Hamahashi, and S. Hina (2012), Tectonic mélange as fault rock of subduction plate boundary, *Tectonophysics*, *568*, 25–38.

Kitajima, H., and D. M. Saffer (2012), Elevated pore pressure and anomalously low stress in regions of low frequency earthquakes along the Nankai Trough subduction megathrust, *Geophys. Res. Lett.*, *39*, L23301, doi:10.1029/2012GL053793.

Kopf, A. (1999), Fate of sediment during plate convergence at the Mediterranean Ridge accretionary complex: Volume balance of mud extrusion versus subduction and/or accretion, *Geology*, *27*, 87.

Kodaira, S., T. Iidaka, A. Kato, J. O. Park, T. Iwasaki, and Y. Kaneda (2004), High pore fluid pressure may cause silent slip in the Nankai Trough, *Science*, *304*(5675), 1295–1298.

Lauer, R. M., and D. M. Saffer (2015), The impact of splay faults on fluid flow, solute transport, and pore pressure distribution in subduction zones: A case study offshore the Nicoya Peninsula, Costa Rica, *Geochem. Geophys. Geosyst.*, *16*, 1089–1104, doi:10.1002/2014GC005638.

Lavier, L. L., R. A. Bennett, R. Duddu (2013), Creep events at the brittle ductile transition, *Geochem. Geophys.*, *14*, 3334–3351.

Leeman, J., D. Saffer, M. Scuderi, and C. Marone (2016), Laboratory observations of slow earthquakes and the spectrum of tectonic fault slip modes, *Nat. Commun.*, *7*, doi:10.1038/ncomms11104.

Lewis, K. B., and J. R. Pettinga (1993), The emerging imbricate frontal wedge of the Hikurangi Margin, in *Basins of the Southwest Pacific. Sedimentary Basins of the World 3*, edited by P. F. Balance, pp. 225–250, Elsevier, Amsterdam.

Liu, Y., and J. R. Rice (2005), Aseismic slip transients emerge spontaneously in three-dimensional rate and state modeling of subduction earthquake sequences, *J. Geophys. Res.*, *110*, B08307, doi:10.1029/2004JB003424.

MacDonald, I., I. Leifer, R. Sassen, P. Stine, R. Mitchell, and N. Guinasso (2002), Transfer of hydrocarbons from natural seeps to the water column and atmosphere, *Geofluids*, *2*(2), 95–107.

Mallick, S., and L. N. Frazer (1987), Practical aspects of reflectivity modeling, *Geophysics*, *52*(10), 1355–1364.

Moore, G. F., D. Saffer, M. Studer, and P. C. Pisani (2011), Structural restoration of thrusts at the toe of the Nankai Trough accretionary prism off Shikoku Island, Japan: Implications for dewatering processes, *Geochem. Geophys. Geosyst.*, *12*, Q0AD12, doi:10.1029/2010GC003453.

Moore, J. C., and P. Vrolijk (1992), Fluids in accretionary prisms, *Rev. Geophys.*, *30*(2), 113–135.

Mountjoy, J. J., and P. M. Barnes (2011), Active upper plate thrust faulting in regions of low plate interface coupling, repeated slow slip events, and coastal uplift: Example from the Hikurangi Margin, New Zealand, *Geochem. Geophys. Geosyst.*, *12*, Q01005, doi:10.1029/2010GC003326.

Nicol, A., and J. Beavan (2003), Shortening of an overriding plate and its implications for slip on a subduction thrust, central Hikurangi Margin, New Zealand, *Tectonics*, *22*(6), 1070.

Pecher, I. A., S. A. Henrys, W. T. Wood, N. Kukowski, G. J. Crutchley, M. Fohrmann, J. Kilner, K. Senger, A. R. Gorman, and R. B. Coffin (2010), Focussed fluid flow on the Hikurangi Margin, New Zealand–Evidence from possible local upwarping of the base of gas hydrate stability, *Mar. Geol.*, *272*, 99–113.

Peng, Z., and J. Gomberg (2010), An integrated perspective of the continuum between earthquakes and slow-slip phenomena, *Nat. Geosci.*, *3*(9), 599–607.

Pettinga, J. R. (1982), Upper Cenozoic structural history, coastal southern Hawke's Bay, New Zealand, *N. Z. J. Geol. Geophys.*, *25*(2), 149–191.

Plaza-Faverola, A., D. Klaeschen, P. Barnes, I. Pecher, S. Henrys, and J. Mountjoy (2012), Evolution of fluid expulsion and concentrated hydrate zones across the southern Hikurangi subduction margin, New Zealand: An analysis from depth migrated seismic data, *Geochem. Geophys. Geosyst.*, *13*, Q08018, doi:10.1029/2012GC004228.

Plaza-Faverola, A., I. Pecher, G. Crutchley, P. M. Barnes, S. Bünz, T. Golding, D. Klaeschen, C. Papenberg, and J. Bialas (2014), Submarine gas seepage in a mixed contractional and shear deformation regime: Cases from the Hikurangi oblique-subduction margin, *Geochem. Geophys. Geosyst.*, *15*, 416–433, doi:10.1002/2013GC005082.

Ranero, C. R., I. Grevemeyer, H. Sahling, U. Barckhausen, C. Hensen, K. Wallmann, W. Weinrebe, P. Vannucchi, R. Von Huene, and K. McIntosh (2008), Hydrogeological system of erosional convergent margins and its influence on tectonics and interplate seismogenesis, *Geochem. Geophys. Geosyst.*, *9*, Q03S04, doi:10.1029/2007GC001679.

Rowe, C. D., J. C. Moore, F. Remitti, and t. I. E. T. Scientists (2013), The thickness of subduction plate boundary faults from the seafloor into the seismogenic zone, *Geology*, *41*(9), 991–994, doi:10.1130/g34556.1.

Saffer, D. M. (2003), Pore pressure development and progressive dewatering in underthrust sediments at the Costa Rican subduction margin: Comparison with northern Barbados and Nankai, *J. Geophys. Res.*, *108*(B5), 2261, doi:10.1029/2002JB001787.

Saffer, D. M., and B. A. Bekins (1999), Fluid budgets at convergent plate margins: Implications for the extent and duration of fault-zone dilation, *Geology*, *27*(12), 1095–1098.

Saffer, D. M., and L. M. Wallace (2015), The frictional, hydrologic, metamorphic and thermal habitat of shallow slow earthquakes, *Nature Geosci.*, *8*, 594–600.

Scholz, C. H., and J. Campos (2012), The seismic coupling of subduction zones revisited, *J Geophys Res-Sol EA.*, *117*(85), doi:10.1029/2011JB009003.

Shipley, T. H., G. F. Moore, N. L. Bangs, J. C. Moore, and P. L. Stoffa (1994), Seismically inferred dilatancy distribution, northern Barbados Ridge decollement: Implications for fluid migration and fault strength, *Geology*, *22*(5), 411–414.

Sibson, R. H. (1994), Crustal stress, faulting and fluid flow, *Geol. Soc. Spec. Publ.*, *78*(1), 69–84.

Sibson, R. H. (2013), Stress switching in subduction forearcs: Implications for overpressure containment and strength cycling on megathrusts, *Tectonophysics*, *600*, 142–152.

Skarbek, R., A. Rempel, D. Schmidt (2012), Geologic heterogeneity can produce aseismic slip transients, *Geophys. Res. Lett.*, *39*(21), doi:10.1029/2012GL053762.

Song, T.-R. A., D. V. Helmberger, M. R. Brudzinski, R. W. Clayton, P. Davis, X. Perez-Campos, and S. K. Singh (2009), Subducting slab ultra-slow velocity layer coincident with silent earthquakes in Southern Mexico, *Science*, *324*(5926), 502–506, doi:10.1126/science.1167595.

Solomon, E. A., M. Kastner, C. G. Wheat, H. Jannasch, G. Robertson, E. E. Davis, and J. D. Morris (2009), Long-term hydrogeochemical records in the oceanic basement and forearc prism at the Costa Rica subduction zone, *Earth Planet. Sci. Lett.*, *282*, 240–251.

Svensen, H., S. Planke, A. Malthe-Sørenssen, B. Jamtveit, R. Myklebust, T. R. Eidem, and S. S. Rey (2004), Release of methane from a volcanic basin as a mechanism for initial Eocene global warming, *Nature*, *429*(6991), 542–545.

Vannucchi, P., F. Sage, J. P. Morgan, F. Remitti, and J. Y. Collot (2012), Toward a dynamic concept of the subduction channel at erosive convergent margins with implications for interplate material transfer, *Geochem. Geophys. Geosyst.*, *13*, Q02003, doi:10.1029/2011GC003846.

Wallace, L. M., J. Beavan, (2010), Diverse slow slip behavior at the Hikurangi subduction margin, New Zealand, *J. Geophys. Res-Sol. EA*, *115*(B12), doi:10.1029/2010JB007717.

Wallace, L. M., J. Beavan, S. Bannister, and C. Williams (2012), Simultaneous long-term and short-term slow slip events at the Hikurangi subduction margin, New Zealand: Implications for processes that control slow slip event occurrence, duration, and migration, *J. Geophys. Res.*, *117*, B11402, doi:10.1029/2012JB009489.

Wallace, L. M., S. C. Webb, Y. Ito, K. Mochizuki, R. Hino, S. Henrys, S. Y. Schwartz, and A. F. Sheehan (2016), Slow slip near the trench at the Hikurangi subduction zone, New Zealand, *Science*, *352*(6286), 701–704, doi:10.1126/science.aaf2349.

Wang, K., S. L. Bilek (2014), Invited review paper: Fault creep caused by subduction of rough seafloor relief, *Tectonophysics*, *610*, 1–24.

Westbrook, G. (1991), Geophysical evidence for the role of fluids in accretionary wedge tectonics, *Philos. Trans. R. Soc. London A*, *335*(1638), 227–242.

Williams, C., D. Eberhart-Phillips, S. Bannister, D. H. N. Barker, S. Henrys, M. Reyners, and R. Sutherland (2013), Revised interface geometry for the Hikurangi Subduction Zone, New Zealand, *Seismol. Res. Lett.*, *84*(6), 1066–1073, doi:10.1785/0220130035.

Wood, R., and B. Davy (1994), The Hikurangi Plateau, *Mar. Geol.*, *118*(1–2), 153–173.